



# Reproducibility of automated calculation technique for diffusion tensor image analysis along the perivascular space

Yuya Saito<sup>1</sup> · Koji Kamagata<sup>1</sup> · Christina Andica<sup>1,2</sup> · Wataru Uchida<sup>1</sup> · Kaito Takabayashi<sup>1</sup> · Seina Yoshida<sup>1,3</sup> · Moto Nakaya<sup>1,4</sup> · Yuya Tanaka<sup>1,4</sup> · Satoru Kamiyo<sup>1,4</sup> · Kanako Sato<sup>1</sup> · Mitsuo Nishizawa<sup>1</sup> · Toshiaki Akashi<sup>1</sup> · Keigo Shimoji<sup>1</sup> · Akihiko Wada<sup>1</sup> · Shigeki Aoki<sup>1</sup>

Received: 14 December 2022 / Accepted: 16 March 2023 / Published online: 10 May 2023  
© The Author(s) under exclusive licence to Japan Radiological Society 2023

## Abstract

**Purpose** The method of diffusion tensor image analysis along the perivascular space (DTI-ALPS) was gathering attention to evaluate the brain's glymphatic function or interstitial fluid dynamics. However, to the best knowledge, no study was conducted on the reproducibility of these automated methods for ALPS index values. Therefore, the current study evaluated the ALPS index reproducibility based on DTI-ALPS using two major automated calculation techniques in scan and rescan of the same subject on the same day.

**Materials and methods** This study included 23 participants, including 2 with Alzheimer's disease, 15 with mild cognitive impairment, and 6 with cognitive normals. Scan and rescan data of diffusion magnetic resonance images were obtained, as well as automatically index for ALPS (ALPS index) and ALPS index maintaining tensor vector orientation information (vALPS index) with region of interest on the template fractional anisotropy map calculated by FSL software. These ALPS indices were compared in terms of scan and rescan reproducibility.

**Results** The absolute difference in ALPS-index values between scan and rescan was larger in the ALPS index than in the vALPS index by approximately 0.6% as the relative difference. Cohen's *d* for the left and right ALPS indices between methods were 0.121 and 0.159, respectively.

**Conclusion** The vALPS index based on DTI-ALPS maintaining tensor vector orientation information has higher reproducibility than the ALPS index. This result encourages a multisite study on the ALPS index with a large sample size and helps detect a subtle pathological change in the ALPS index.

**Keywords** Diffusion magnetic resonance imaging · Diffusion tensor imaging · Along the perivascular space index · Reproducibility · Glymphatic system

## Introduction

The glymphatic system has earned interest since Ilf et al. advocated the system [1]. The glymphatic system plays a role in waste product excretion, including neurotoxins, such as amyloid  $\beta$  ( $A\beta$ ) and tau protein within the brain. A glymphatic system dysfunction could cause extracellular  $A\beta$  accumulation before the onset of dementia and Alzheimer's disease (AD) [1, 2]. Thus, the glymphatic system is an essential  $A\beta$  clearance component in the brain of rodents. A tracer study, which is one of the most efficient methods to visualize interstitial fluid dynamics, is the major method to evaluate the glymphatic system. The initial study on the glymphatic system evaluation used a fluorescent tracer and a laser-scanning microscope [1]. The follow-up tracer studies

✉ Koji Kamagata  
kkamagat@juntendo.ac.jp

<sup>1</sup> Department of Radiology, Juntendo University Graduate School of Medicine, Tokyo, Japan

<sup>2</sup> Faculty of Health Data Science, Juntendo University, Chiba, Japan

<sup>3</sup> Department of Radiological Sciences, Graduate School of Human Health Sciences, Tokyo Metropolitan University, Tokyo, Japan

<sup>4</sup> Department of Radiology, University of Tokyo, Tokyo, Japan

used the intrathecal administration of gadolinium-based contrast agent (GBCA) on magnetic resonance imaging (MRI) using animal models, such as a mouse, as the other method [3, 4]. However, such a study using the intrathecal GBCA administration on MRI is invasive for a subject and is accompanied by pain. The intrathecal GBCA administration in humans has not been approved in any country [5]. Therefore, performing the intrathecal GBCA administration for a human subject is difficult.

As a non-invasive method of the glymphatic system without intrathecal contrast agent injection [1, 2], Taoka et al. [6] proposed diffusion tensor image analysis along the perivascular space (DTI-ALPS) based on diffusion MRI (dMRI) which non-invasively evaluates the interstitial fluid dynamics using DTI on MRI. The DTI-ALPS method provides the ALPS index, which is a ratio of the perivascular space direction diffusivity and perpendicular major fiber tract and perivascular space direction diffusivity [6, 7]. Recently, the DTI-ALPS method was reported to reflect the glymphatic system alteration of intestinal fluid dynamics in various pathologies [8–15]. These reports suggest the usefulness of the ALPS index as a biomarker to evaluate interstitial fluid dynamics or glymphatic function. However, these ALPS index calculation methods were manual region of interest (ROI) placement, which cost a lot in terms of time and human resources. Therefore, introducing manual volumetric assessments in clinical settings is difficult. Thus, automated calculation techniques for the ALPS index have been developed, such as ALPS index [14] and ALPS index maintaining tensor vector orientation information (vALPS index), to overcome this problem [16, 17]. However, to the best knowledge, the reproducibility of these automated methods for ALPS index values was not studied.

Therefore, the current study evaluated the reproducibility of the ALPS index values based on DTI-ALPS using ALPS and vALPS indices in scan and rescan of the same subject on the same day.

## Materials and Methods

### Study cohorts

Data used in this study were obtained from the Alzheimer's Disease Neuroimaging Initiative (ADNI)-3 database (<https://adni.loni.usc.edu>). ADNI was launched in 2003 as a public–private partnership, led by principal investigator Michael W. Weiner, MD, VA Medical Center and University of California, San Francisco. ADNI primarily aimed to test whether serial MRI, positron emission tomography, other biological markers, and clinical and neuropsychological assessment can be combined to measure the progression of mild cognitive

**Table 1** Participant demographic data

	<i>n</i>	23
Age, y		69.9 ± 6.3
Sex, male/female		13/10
Education, y		16.3 ± 2.6
Race		White
CN/MCI/AD		6/15/2
MMSE		27.4 ± 2.5
MoCA		24.2 ± 4.6
CDR-SB		1.1 ± 1.2
FAQ		2.2 ± 3.2

CN cognitive normal, MCI mild cognitive impairment, AD Alzheimer's disease, MMSE Mini-Mental State Examination, MoCA Montreal Cognitive Assessment, CDR-SB Clinical Dementia Rating Sum of Boxes, FAQ Functional Activities Questionnaire

impairment (MCI) and early AD. See [www.adni-info.org](http://www.adni-info.org) for a more detailed and up-to-date ADNI description.

The current study included 23 participants (2 AD, 15 MCI, and 6 cognitive normals [CNs]) with clinical neuropsychological scores and two dMR images (i.e., scan and rescan) on the same day from the ADNI-3 database. A 3 Tesla MRI scanner, including Prisma fit (Siemens Healthineers, Erlangen, Germany) with a single protocol, was used to obtain dMRI data. Table 1 shows the demographic and clinical data of study participants.

### Neuropsychological assessments

This study collected the following neuropsychological tests: Mini-Mental State Examination (MMSE) [18]; Montreal cognitive assessment (MoCA) [19], a brief questionnaire that measures global cognitive impairment; clinical dementia rating scale sum of boxes (CDR-SB); functional activities questionnaire (FAQ), an assessment which rates patients' ability to independently complete activities of daily living [20].

### MRI acquisition

Scan and rescan dMRI was acquired for each participant using a 3 Tesla Siemens Prisma fit scanner. More imaging details are found at <http://adni.loni.usc.edu/methods/documents/mri-protocols/>.

In brief, the following parameters were used for Prisma fit:  $b = 0/1000 \text{ s/mm}^2$ ; non-diffusion-weighted image = 7; 48 MPG axes; repetition time (TR) = 7200 ms; TE = 56.0; flip angle 90°; 2.00 mm isotropic voxel; and 55 axial slices.

### dMRI processing

FSL 6.0.1 and MRtrix3, following recent studies on optimal preprocessing, were used to preprocess acquired dMRI data [21]. First, Marchenko–Pastur principal component analysis (MP-PCA), as a denoise algorithm, [22] and Gibbs artifacts, were used to denoise and correct MR magnitude images [23]. Next, an analytical approach was adopted and the noise standard deviation estimated by applying MP-PCA was used to reduce possible biases caused by Rician noise distribution. Additionally, the “eddy” commands in the FSL software and B1 inhomogeneity were used to correct the effects of eddy currents and motion, including dMR images [24]. Then, the resulting dMR images were fitted to the DTI model based on estimation with ordinary least squares to generate FA and diffusion coefficient maps (i.e., diffusion tensor image) in the x-axis (right-left; D<sub>xx</sub>), y-axis (anterior–posterior; D<sub>yy</sub>), and z-axis (inferior-superior; D<sub>zz</sub>) directions using the “dtifit” command in the FSL software [25]. Finally, the diffusion coefficient and FA maps were assessed to determine whether the data were free from severe artifacts, such as gross geometric distortion, signal dropout, and bulk motion.

### Along the perivascular space index calculation

The ALPS-index based on DTI-ALPS was automatically calculated according to two methods, including ALPS index [14] and vALPS index [16, 17] (Fig. 1).

First, the FA maps of all participants were registered linearly and then non-linearly into the high-resolution FMRIB58\_FA template-space image (1-mm isotropic voxel). Second, this transformation matrix from subject

to template space was used to register diffusion coefficient maps to the FA template. Third, four 5-mm-diameter ROIs were placed in the projection and association areas at the level of the lateral ventricle bodies in the left and right hemispheres on the FA template. Dominant fibers run in the z-axis direction, perpendicular to both the x- and y-axes in the projection area, whereas dominant fibers run in the y-axis direction, perpendicular to both the x- and z-axes in the association area. Fourth, the resulting ROIs were registered to the same FA template. The position of the resulting ROIs in the FA template space was visually checked for each participant. Manual corrections were not performed because all ROIs were correctly placed. Finally, the ALPS index was calculated similarly to the conventional ALPS index as follows:

$$ALPS\ index = \frac{\text{mean}(D_{xxproj}, D_{xxassoc})}{\text{mean}(D_{yyproj}, D_{zzassoc})}, \tag{1}$$

which is a ratio of the mean of the x-axis diffusivity in the projection area ( $D_{xxproj}$ ) and x-axis diffusivity in the association area ( $D_{xxassoc}$ ) to the mean of the y-axis diffusivity in the projection area ( $D_{yyproj}$ ) and the z-axis diffusivity in the association area ( $D_{zzassoc}$ ). ALPS index close to 1.0 reflects minimal diffusivity along the perivascular space, whereas a higher value indicates greater diffusivity.

These maps were registered using the “vecreg” function implemented in FSL to preserve orientation information after registering diffusion coefficient maps to the FA template for the vALPS calculation. Then, vALPS was calculated according to the above formula (1).

### Statistical analysis

The absolute difference between the ALPS index of scan and rescan and the relative difference of rescan compared to scan (i.e., the first scan) was calculated to evaluate reproducibility for each automated ALPS index calculation method. Moreover, Cohen’s *d* effect size of the ALPS index between scan and rescan was calculated. To compare the difference between ALPS and vALPS index, Cohen’s *d* formula can be described as follows:

$$S_c = \sqrt{\frac{n_1 S_1^2 + n_2 S_2^2}{n_1 n_2}} \tag{2}$$

$$\text{Cohen's } d = \frac{|\bar{x}_1 - \bar{x}_2|}{S_c}, \tag{3}$$

where  $n_1$  and  $n_2$  represent the numbers of subjects in populations 1 and 2, respectively;  $\bar{x}_1$  and  $\bar{x}_2$  and  $S_1$  and  $S_2$  represent the average and standard deviation of the

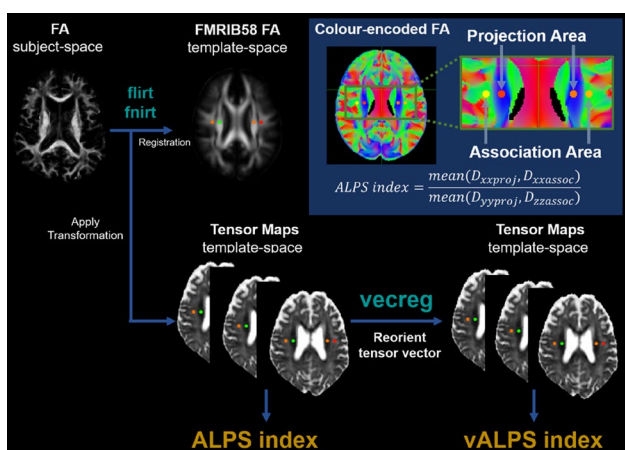


**Fig. 1** The procedure of automated ALPS index calculation. The ALPS index based on DTI-ALPS was automatically calculated according to two methods, including ALPS index and ALPS index maintaining tensor vector orientation information (vALPS index)

absolute difference of ALPS and vALPS index between scan and rescans, respectively. This formula indicates that the difference of reproducibility between ALPS and vALPS index in scan and rescans as Cohen’s *d* is small.

**Table 2** Comparison of automated ALPS index calculation methods

	ALPS index	vALPS index
Mean absolute difference [relative difference, %]		
<b>Left</b>		
$D_{xxproj}$	$1.68 \times 10^{-5}$ [2.80]	$1.69 \times 10^{-5}$ [2.81]
$D_{xxassoc}$	$3.17 \times 10^{-5}$ [3.70]	$3.07 \times 10^{-5}$ [3.64]
$D_{yyproj}$	$1.74 \times 10^{-5}$ [3.78]	$1.57 \times 10^{-5}$ [3.52]
$D_{zzassoc}$	$1.19 \times 10^{-5}$ [2.59]	$1.37 \times 10^{-5}$ [1.59]
ALPS index	$2.63 \times 10^{-2}$ [1.66]	$1.75 \times 10^{-2}$ [1.06]
<b>Right</b>		
$D_{xxproj}$	$1.69 \times 10^{-5}$ [2.99]	$1.68 \times 10^{-5}$ [2.98]
$D_{xxassoc}$	$2.29 \times 10^{-5}$ [2.78]	$2.30 \times 10^{-5}$ [2.79]
$D_{yyproj}$	$1.72 \times 10^{-5}$ [3.76]	$1.57 \times 10^{-5}$ [3.52]
$D_{zzassoc}$	$1.32 \times 10^{-5}$ [2.52]	$1.29 \times 10^{-5}$ [2.34]
ALPS index	$3.73 \times 10^{-2}$ [2.55]	$3.31 \times 10^{-2}$ [2.28]

A comparison between automated ALPS index calculation methods in the left (left ALPS index) and right hemispheres (right ALPS index). The mean absolute difference between the ALPS index of scan and rescans and the mean relative difference of rescans compared with scan (i.e., the first scan) was calculated to evaluate the reproducibility of each automated ALPS index calculation method

Automated calculation techniques for ALPS-index have been developed such as ALPS index and ALPS-index maintaining tensor vector orientation information (vALPS index)

Additionally, to confirm the reproducibility of the correlation between ALPS index and clinical score, such as MMSE, MoCA, CDR-SB, and FAQ, the absolute difference between scan and rescans of the partial correlation between ALPS index and clinical score with covariates, including age, sex, and years of education, was calculated.

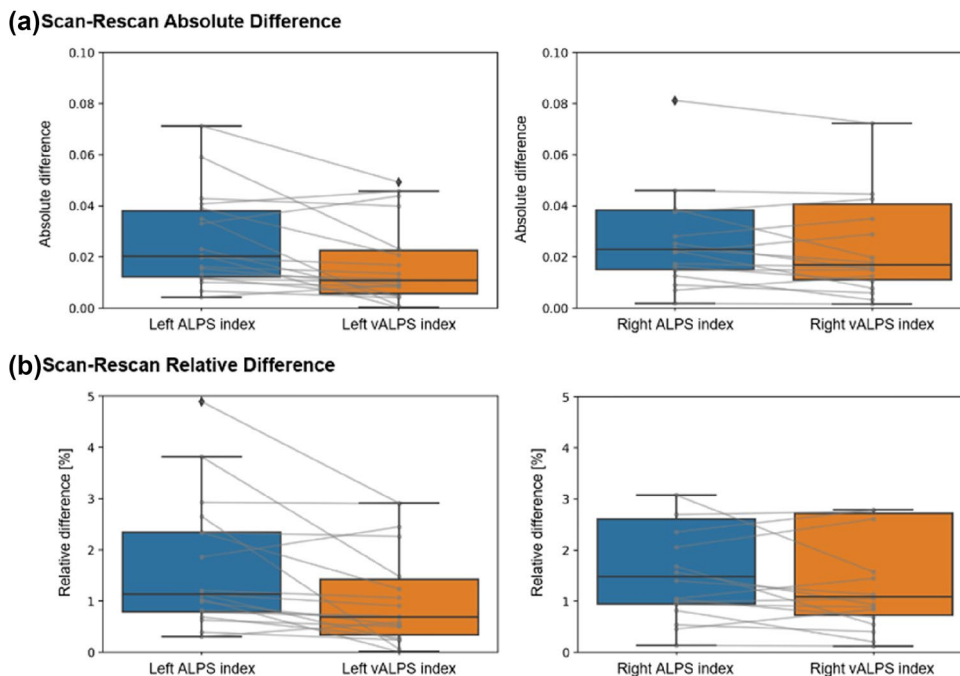
**Results**

Table 2 and Fig. 2 show the result of a comparison between automated ALPS index calculation methods in the left (left ALPS index) and right hemisphere (right ALPS index). The absolute difference in almost diffusivity and the ALPS index between scan and rescans was larger in the ALPS index than the vALPS index by approximately 0.6% as the relative difference of ALPS index. Cohen’s *d* for the left and right ALPS indices between methods were 0.121 and 0.159, respectively. On the other hand, the absolute difference of correlation of ALPS index and clinical score between scan and rescans was lower in the vALPS index (Table 3).

**Discussion**

The current study evaluated the reproducibility of the ALPS index, such as ALPS and vALPS indices, and the difference of the ALPS index between scan and rescans and the relative difference of rescans compared to scan were calculated. The result revealed that the absolute difference in the ALPS index between scan and rescans was larger in the ALPS index

**Fig. 2** Comparison of automated ALPS index calculation methods. Boxplots showing the difference of ALPS index in the left (left ALPS index) and right hemisphere (right ALPS index) between automated ALPS-index calculation methods in scan (blue) and rescans (red). The boxplots represent the interquartile ranges, which contain 50% of individual subjects’ values. The whiskers are lines that extend from the box to the highest and lowest values. Abbreviation: automated calculation techniques for ALPS index have been developed such as ALPS index and ALPS index maintaining tensor vector orientation information (vALPS index)



**Table 3** Absolute difference in the correlation between scan and rescan

	MMSE	MoCA	CDRSB	FAQ
Left				
ALPS index	0.01	0.16	0.11	0.04
vALPS index	0.01	0.09	0.09	0.07
Right				
ALPS index	0.03	0.17	0.16	0.09
vALPS index	0.01	0.14	0.12	0.06

Absolute difference between scan and rescan of the partial correlation of the ALPS index and clinical score with covariances, including age, sex, and years of education, was calculated

*MMSE* Mini-Mental State Examination, *MoCA* Montreal Cognitive Assessment, *CDR-SB* Clinical Dementia Rating Sum of Boxes, *FAQ* Functional Activities Questionnaire

than in the vALPS index. Additionally, Cohen’s *d* for the left and right ALPS indices between methods were 0.121 and 0.159, respectively, which means a small effect size according to Cohen’s *d* guideline [26]. Furthermore, vALPS index had lower absolute difference of correlation with clinical score between scan and rescan than ALPS index.

Taoka et al. [27] investigated the reproducibility of the ALPS index, including the ALPS index of DTI-ALPS regarding test–retest. The absolute difference among ALPS indices of four times scans in the test–retest study was up to approximately 0.02. This result was consistent with the absolute difference of the ALPS index in our study. Conversely, the absolute difference between the vALPS index was lower than that of the ALPS index. The vALPS index maintains the tensor vector orientation information. Figure 3 shows three types of color-encoded fractional anisotropy (FA) images: left, color-encoded FA in the subject’s space;

middle, registered one in the template space without tensor vector reorientation; right, registered one in the template space with tensor vector reorientation using the “vecreg” function implemented in the FSL library. The application of spatial transformations to diffusion tensor images is complicated because the diffusion tensor images contain orientational information, which is affected by the transformation, compared to the task of warping scalar images, as shown in Fig. 3. This effect should be accounted for to ensure the anatomical correctness of the transformed image. Alexander et al. [28] revealed that accompanying reorientation of the data is required to preserve the consistency of the data concerning the anatomic structure of the image when transformations are applied to a diffusion tensor image. The transformation matrix, normalized for scaling, can be directly applied to each diffusion tensor in the image, via a similarity transform, to perform the necessary reorientation for rigid rotation and/or uniform scaling. Indeed, the vALPS index also had lower absolute difference of correlation with clinical score between scan and rescan than the ALPS index. It implies that the vALPS index is superior over the ALPS index in the reproducibility of the correlation with clinical scores and its index value. Thus, the vALPS index, maintaining tensor vector orientation information, had higher reproducibility than the ALPS index without consideration.

Recently, Tatekawa et al. [29] also attempted to improve the reproducibility of the DTI-ALPS index and to evaluate whether the reorientation of DTI data (i.e., vALPS index) improved the reproducibility of the ALPS index with manual ROI placement using 234 cognitively healthy subjects from the OASIS-3 dataset. The literature showed that the vALPS index exhibited a significantly smaller variance than the original ALPS index ( $p < 0.001$ ). For intra- and inter-reliability, the vALPS index indicated better reproducibility

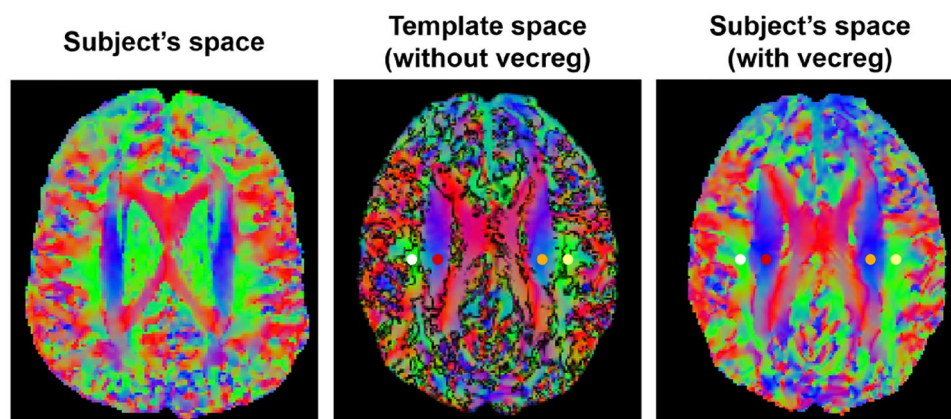


**Fig. 3** The difference between registrations with and without tensor vector reorientation. Three types of color-encoded fractional anisotropy (FA) images were shown. Left, color-encoded FA in subject’s space; middle, registered one in the template space without tensor

vector reorientation; right, registered one in the template space with tensor vector reorientation using the “vecreg” function implemented in the FSL library. Red and orange ROIs are in the association area, and white and yellow ROIs are in the projection area

than the original ALPS index, even in subjects with head rotation (ICCs of original ALPS index: 0.52–0.81; ICCs of vALPS index: > 0.85). A wider range of the 95% limit of agreement of the Bland–Altman plot for subjects with X-axis rotation was identified, indicating that X-axis rotation remarkably affected the calculation of the ALPS index. Although there is a little difference between our studies in terms of manual or automated ROI placement, our results that the vALPS index has better reproducibility than the original ALPS index, were consistent with those of a previous study.

The absolute difference in the ALPS index was compared with the change of the ALPS index in some diseases in the previous report to confirm the effect of improved ALPS index reproducibility. The absolute difference in the ALPS index between CN and MCI, CN and AD, and MCI and AD was 0.05, 0.04, and 0.01, respectively, in MCI and AD [10]. The ALPS index of Parkinson's disease (PD) with MCI (PD-MCI) decreased by 0.02 compared to PD with cognitive normal (PD-CN) [9]. Additionally, the ALPS index of PD with dementia was lower than PD-MCI by 0.05. Furthermore, the ALPS index of early PD was lower than late PD by 0.05. McKnight et al. [30] showed Cohen's *d* between PD and essential tremor was 0.19, while Cohen's *d* between healthy males and females was 0.21. Conversely, the Cohen's *d* between CN and MCI, CN and AD, and MCI and AD were 0.29, 0.22, and 0.07, respectively. A study on the human immunodeficiency virus (HIV) indicated a lower ALPS index in HIV than in healthy controls by 0.02 [31]. Cohen's *d* was 0.12 in the comparison between patients with migraine with and without aura [32]. Lee et al. [33] reported that the ALPS index in transient global amnesia was higher than healthy controls and Cohen's *d* was 0.14. The reproducibility of scan and rescan was higher in the vALPS index, and the effect size (i.e., Cohen's *d*) of method difference for the ALPS index calculation is almost the same as or larger than that of the subtle pathological change reported in the above studies, considering our study that revealed Cohen's *d* between ALPS and vALPS indices for the left and right of 0.121 and 0.159, respectively. Hence, the vALPS index could be used to detect subtle pathological changes with a small effect size.

This study has some limitations. First, the sample size was small. Hence, a larger sample size was desired to improve the statistical power and reliability of the results. However, to the best of our knowledge, no open database with a large sample is available, (e.g., such as ADNI (<https://adni.loni.usc.edu/>), Human Connectome Project (<https://db.humanconnectome.org/>), Open Access Series of Imaging Studies (<https://www.oasis-brains.org/>), 4-Repeat Tauopathy Neuroimaging Initiative, and the Frontotemporal Lobar Degeneration Neuroimaging Initiative (<http://4rtmi-ftldni.ini.usc.edu/>)) of scan and rescan MRI obtained at the same day. In this study,

absolute difference between scan and rescan was lower in the vALPS index than in the ALPS index, and the effect sizes were 0.121 and 0.159 as Cohen's *d* for the left and right ALPS indices, respectively. If the false-positive error (i.e.,  $\alpha$  error) is 0.05 and statistical power (i.e.,  $1-\beta$ ) is 0.80, the required total sample size is at least 539 to statistically show that the absolute difference of the vALPS index is significantly lower than that of the ALPS index. Second, MRI data were obtained using a single scanner, in a single institution. Thus, evaluating the reproducibility of automated ALPS index calculation methods using various conditions, including multi-scanner and protocol, is desirable. Third, the current study did not stratify the patients and healthy controls. Therefore, investigating the reproducibility of ALPS and vALPS indices while separating patients and control participants can help deepen understanding of the reproducibility of the ALPS index. However, automated methods for calculating the ALPS index might be required to avoid the subjectivity caused by manual ROI placement and the cost, such as human resources and time consumption, and achieve the study, because the multisite study on the glymphatic system using the ALPS index, targeting large sample size, is gaining interest. Our study revealed the effect of the difference between automated methods for the ALPS index calculation.

In conclusion, the vALPS index based on DTI-ALPS maintaining tensor vector orientation information has higher reproducibility than the ALPS index. This result could encourage a multisite study on the ALPS index with a large sample size and lead to detect subtle pathological changes in the ALPS index.

**Acknowledgements** This work was supported by JSPS KAKENHI Grant Number JP22H04926, 18K18164, and 21K12153. Data collection and sharing for this project was funded by the Alzheimer's Disease Neuroimaging Initiative (ADNI) (National Institutes of Health Grant U01 AG024904) and DOD ADNI (Department of Defense award number W81XWH-12-2-0012). ADNI is funded by the National Institute on Aging, the National Institute of Biomedical Imaging and Bioengineering, and through generous contributions from the following: AbbVie, Alzheimer's Association; Alzheimer's Drug Discovery Foundation; Araclon Biotech; BioClinica, Inc.; Biogen; Bristol-Myers Squibb Company; CereSpir, Inc.; Cogstate; Eisai Inc.; Elan Pharmaceuticals, Inc.; Eli Lilly and Company; EuroImmun; F. Hoffmann-La Roche Ltd and its affiliated company Genentech, Inc.; Fujirebio; GE Healthcare; IXICO Ltd.; Janssen Alzheimer Immunotherapy Research & Development, LLC.; Johnson & Johnson Pharmaceutical Research & Development LLC.; Lumosity; Lundbeck; Merck & Co., Inc.; Meso Scale Diagnostics, LLC.; NeuroRx Research; Neurotrack Technologies; Novartis Pharmaceuticals Corporation; Pfizer Inc.; Piramal Imaging; Servier; Takeda Pharmaceutical Company; and Transition Therapeutics. The Canadian Institutes of Health Research is providing funds to support ADNI clinical sites in Canada. Private sector contributions are facilitated by the Foundation for the National Institutes of Health ([www.fnih.org](http://www.fnih.org)). The grantee organization is the Northern California Institute for Research and Education, and the study is coordinated by the Alzheimer's Therapeutic Research Institute at the University of

Southern California. ADNI data are disseminated by the Laboratory for Neuro Imaging at the University of Southern California.

**Funding** Data collection and sharing for this project were funded by the ADNI (National Institutes of Health grant no. U01 AG024904) and Department of Defense ADNI (Department of Defense award number W81XWH-12-2-0012). This study was partially supported by the Juntendo Research Branding Project, JSPS KAKENHI I (grant nos. 16H06280, 18K18164, 18H02772, 19K17244, 21K07690, 21K12153, 22H04926, 23H02865), a Grant-in-Aid for Special Research in Subsidies for ordinary expenses of private schools from The Promotion and Mutual Aid Corporation for Private Schools of Japan, the Brain/MINDS Beyond program (grant no. JP19dm0307101) of the Japan Agency for Medical Research and Development (AMED), and AMED under grant number JP21wm0425006.

#### Declaration

**Ethical approval** This article used open-source data from the ADNI 3 brain project (<https://adni.loni.usc.edu/adni-3/>) and did not involve studies with human participants or animals performed by the authors at our institution.

## References

- Iliff JJ, Wang M, Liao Y, Plogg BA, Peng W, Gundersen GA, et al. A paravascular pathway facilitates CSF flow through the brain parenchyma and the clearance of interstitial solutes, including amyloid  $\beta$ . *Sci Transl Med*. 2012;4:147ra111.
- Kress BT, Iliff JJ, Xia M, Wang M, Wei HS, Zeppenfeld D, et al. Impairment of paravascular clearance pathways in the aging brain. *Ann Neurol*. 2014;76:845–61.
- Gabriel T, Gakuba C, Goulay R, Martinez De Lizarrondo S, Hanouz J-L, Emery E, et al. Impaired glymphatic perfusion after strokes revealed by contrast-enhanced MRI: a new target for fibrinolysis? *Stroke*. 2014;45:3092–6.
- Iliff JJ, Lee H, Yu M, Feng T, Logan J, Nedergaard M, et al. Brain-wide pathway for waste clearance captured by contrast-enhanced MRI. *J Clin Invest*. 2013;123:1299–309.
- Siebner HR, von Einsiedel HG, Conrad B. Magnetic resonance ventriculography with gadolinium DTPA: report of two cases [Internet]. *Neuroradiology*. 1997. <https://doi.org/10.1007/s002340050436>.
- Taoka T, Masutani Y, Kawai H, Nakane T, Matsuoka K, Yasuno F, et al. Evaluation of glymphatic system activity with the diffusion MR technique: diffusion tensor image analysis along the perivascular space (DTI-ALPS) in Alzheimer's disease cases. *Jpn J Radiol*. 2017;35:172–8.
- Taoka T, Fukusumi A, Miyasaka T, Kawai H, Nakane T, Kichikawa K, et al. Structure of the medullary veins of the cerebral hemisphere and related disorders. *Radiographics*. 2017;37:281–97.
- Bae YJ, Choi BS, Kim J-M, Choi J-H, Cho SJ, Kim JH. Altered glymphatic system in idiopathic normal pressure hydrocephalus. *Parkinsonism Relat Disord*. 2021;82:56–60.
- Chen H-L, Chen P-C, Lu C-H, Tsai N-W, Yu C-C, Chou K-H, et al. Associations among cognitive functions, plasma DNA, and diffusion tensor image along the perivascular space (DTI-ALPS) in patients with Parkinson's disease. *Oxid Med Cell Longev*. 2021;2021:4034509.
- Steward CE, Venkatraman VK, Lui E, Malpas CB, Ellis KA, Cyarto EV, et al. Assessment of the DTI-ALPS parameter along the perivascular space in older adults at risk of dementia. *J Neuroimaging*. 2021;31:569–78.
- Toh CH, Castillo M. Peritumoral brain edema volume in meningioma correlates with tumor fractional anisotropy but not apparent diffusion coefficient or cerebral blood volume. *Neuroradiology*. 2021;63:1263–70.
- Yang G, Deng N, Liu Y, Gu Y, Yao X. Evaluation of glymphatic system using diffusion MR technique in T2DM cases. *Front Hum Neurosci*. 2020;14:300.
- Yokota H, Vijayasarathi A, Cekic M, Hirata Y, Linetsky M, Ho M, et al. Diagnostic performance of glymphatic system evaluation using diffusion tensor imaging in idiopathic normal pressure hydrocephalus and mimickers. *Curr Gerontol Geriatr Res*. 2019;2019:5675014.
- Zhang W, Zhou Y, Wang J, Gong X, Chen Z, Zhang X, et al. Glymphatic clearance function in patients with cerebral small vessel disease. *Neuroimage*. 2021;238: 118257.
- Zhou W, Shen B, Shen W-Q, Chen H, Zheng Y-F, Fei J-J. Dysfunction of the glymphatic system might be related to iron deposition in the normal aging brain. *Front Aging Neurosci*. 2020;12: 559603.
- Zhang Y, Zhang R, Ye Y, Wang S, Jiaerken Y, Hong H, et al. The influence of demographics and vascular risk factors on glymphatic function measured by diffusion along perivascular space. *Front Aging Neurosci*. 2021;13: 693787.
- Carotenuto A, Cacciaguerra L, Pagani E, Preziosa P, Filippi M, Rocca MA. Glymphatic system impairment in multiple sclerosis: relation with brain damage and disability. *Brain Oxf Acad*. 2021;145:2785–95.
- Folstein MF, Folstein SE, McHugh PR. "Mini-mental state". A practical method for grading the cognitive state of patients for the clinician. *J Psychiatr Res*. 1975;12:189–98.
- Nasreddine ZS, Phillips NA, Bédirian V, Charbonneau S, Whitehead V, Collin I, et al. The Montreal Cognitive Assessment, MoCA: a brief screening tool for mild cognitive impairment. *J Am Geriatr Soc*. 2005;53:695–9.
- Pfeffer RI, Kurosaki TT, Harrah CH Jr, Chance JM, Filos S. Measurement of functional activities in older adults in the community. *J Gerontol*. 1982;37:323–9.
- Tournier J-D, Smith R, Raffelt D, Tabbara R, Dhollander T, Pietsch M, et al. MRtrix3: a fast, flexible and open software framework for medical image processing and visualisation. *Neuroimage*. 2019;202: 116137.
- Cordero-Grande L, Christiaens D, Hutter J, Price AN, Hajnal JV. Complex diffusion-weighted image estimation via matrix recovery under general noise models. *Neuroimage*. 2019;200:391–404.
- Kellner E, Dhital B, Kiselev VG, Reiser M. Gibbs-ringing artifact removal based on local subvoxel-shifts. *Magn Reson Med*. 2016;76:1574–81.
- Graham MS, Drobnjak I, Jenkinson M, Zhang H. Quantitative assessment of the susceptibility artefact and its interaction with motion in diffusion MRI. *PLoS ONE*. 2017;12: e0185647.
- Jenkinson M, Beckmann CF, Behrens TEJ, Woolrich MW, Smith SM. FSL. *Neuroimage*. 2012;62:782–90.
- Cohen J. A power primer. *Psychol Bull*. 1992;112:155–9.
- Taoka T, Ito R, Nakamichi R, Kamagata K, Sakai M, Kawai H, et al. Reproducibility of diffusion tensor image analysis along the perivascular space (DTI-ALPS) for evaluating interstitial fluid diffusivity and glymphatic function: CHanges in Alps index on Multiple condition acquisition eXperiment (CHAMONIX) study. *Jpn J Radiol*. 2022;40:147–58.
- Alexander DC, Pierpaoli C, Basser PJ, Gee JC. Spatial transformations of diffusion tensor magnetic resonance images. *IEEE Trans Med Imaging*. 2001;20:1131–9.
- Tatekawa H, Matsushita S, Ueda D, et al. Improved reproducibility of diffusion tensor image analysis along the perivascular space

- (DTI-ALPS) index: an analysis of reorientation technique of the OASIS-3 dataset. *Jpn J Radiol.* 2023;41(4):393–400. <https://doi.org/10.1007/s11604-022-01370-2>
30. McKnight CD, Trujillo P, Lopez AM, Petersen K, Considine C, Lin Y-C, et al. Diffusion along perivascular spaces reveals evidence supportive of glymphatic function impairment in Parkinson disease. *Parkinsonism Relat Disord.* 2021;89:98–104.
  31. Nguchu BA, Zhao J, Wang Y, de Dieu UJ, Wang X, Qiu B, et al. Altered glymphatic system in middle-aged cART-treated patients with HIV: a diffusion tensor imaging study. *Front Neurol.* 2022;13: 819594.
  32. Lee DA, Lee H-J, Park KM. Normal glymphatic system function in patients with migraine: A pilot study. *Headache.* 2022;62:718–25.
  33. Lee DA, Park BS, Park S, Lee YJ, Ko J, Park KM. Glymphatic system function in patients with transient global amnesia. *J Integr Neurosci.* 2022;21:117.

**Publisher's Note** Springer Nature remains neutral with regard to jurisdictional claims in published maps and institutional affiliations.

Springer Nature or its licensor (e.g. a society or other partner) holds exclusive rights to this article under a publishing agreement with the author(s) or other rightsholder(s); author self-archiving of the accepted manuscript version of this article is solely governed by the terms of such publishing agreement and applicable law.